Journal Pre-proofs

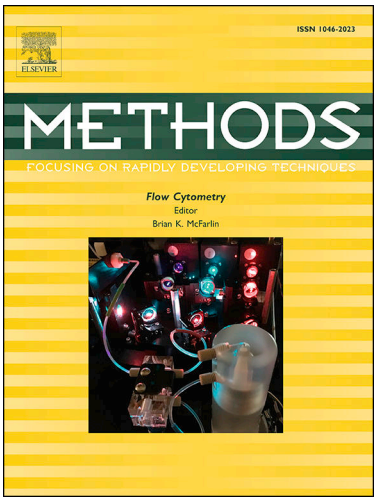

In vivo detection of GPCR-dependent signaling using fiber photometry and FRET-based biosensors

Jace Jones-Tabah, Hanan Mohammad, Paul B.S. Clarke, Terence E. Hébert

PII: S1046-2023(21)00128-6
DOI: https://doi.org/10.1016/j.ymeth.2021.05.002
Reference: YMETH 5078

To appear in: *Methods*

Received Date: 5 April 2021
Revised Date: 3 May 2021
Accepted Date: 11 May 2021

Please cite this article as: J. Jones-Tabah, H. Mohammad, P.B.S. Clarke, T.E. Hébert, *In vivo* detection of GPCR-dependent signaling using fiber photometry and FRET-based biosensors, *Methods* (2021), doi: https://doi.org/10.1016/j.ymeth.2021.05.002

In vivo detection of GPCR-dependent signaling using fiber photometry and FRET-based biosensors

Jace Jones-Tabah, Hanan Mohammad, Paul B.S. Clarke* and Terence E. Hébert*

[1]Department of Pharmacology and Therapeutics, McGill University, Montréal, Québec, H3G 1Y6, Canada

* Co-corresponding authors- send correspondence to:

Dr. Terence E. Hébert, PhD,

Department of Pharmacology and Therapeutics,

McGill University,

3655 Promenade Sir-William-Osler, Room 1325

Montréal, Québec, H3G 1Y6, Canada

Tel: (514) 398-1398

E-mail: terence.hebert@mcgill.ca

OR

Dr. Paul Clarke, PhD,

Department of Pharmacology and Therapeutics,

McGill University,

3655 Promenade Sir-William-Osler, Room 1325

Montréal, Québec, H3G 1Y6, Canada

Tel: (514) 398-3616 ext 1

E-mail: paul.clarke@mcgill.ca

Highlights

- **Methods are described for *in vivo* recording of FRET biosensors using fiber photometry**
- **Technical considerations are discussed for biosensor expression and recording in freely moving animals**
- **Example of detecting GPCR-dependent signaling events in the rat striatum is presented**

Abstract

Genetically encoded fluorescent biosensors allow intracellular signaling dynamics to be tracked in live cells and tissues using optical detection. Many such biosensors are based on the principle of Förster resonance energy transfer (FRET), and we have recently developed a simple approach for *in vivo* detection of FRET-based biosensor signals using fiber photometry. By combining fiber photometry with FRET-based biosensors, we were able to track GPCR-dependent signaling pathways over time, and in response to drug treatments in freely-moving adult rats. Recording from specific neuronal populations, we can quantify intracellular signaling while simultaneously measuring behavioral responses. Our approach, described in detail here, uses adeno-associated viruses infused intracerebrally in order to express genetically-encoded FRET-based biosensors. After several weeks to allow biosensor expression, fiber photometry is used in order to record drug responses in real time from freely-moving adult rats. This methodology would be compatible with other mammalian species and with many biosensors. Hence, it has wide applicability across a spectrum of neuroscience research, ranging from the study of neural circuits and behavior, to preclinical drug development and screening.

1. Introduction

A longstanding obstacle in neuroscience research has been the inability to observe cellular and molecular processes in the brain from subjects that are awake, and hence able to interact with the environment. Over the last decade, fluorescent indicators and advanced imaging modalities have been developed that allow such cellular and molecular processes to be measured in real time from awake animals. The suite of available biosensors now includes indicators of calcium concentration, voltage, second messenger production, enzyme activities, and neurotransmitter or neuromodulator release, and new sensors are being generated routinely. Many such biosensors are constructed by exploiting Förster resonance energy transfer (FRET), which occurs between two fluorescent proteins as a function of their proximity, and is detectable as a change in relative fluorescence intensity or fluorescence lifetime (reviewed in [1-3]). Imaging or recording of such fluorescent biosensors in living animals can be accomplished using several techniques, each with specific advantages (reviewed in [4, 5]). In this article we will outline one such technology, fiber photometry, and its application to FRET-based biosensors.

Fiber photometry refers to an optogenetic technique in which a fiberoptic probe (sometimes referred to as an optic cannula) is chronically implanted in order to record the fluorescence emissions of a biosensor from a target tissue, such as the brain [6-10]. While specific apparati can vary, most fiber photometry systems do not employ cameras for detecting fluorescence and thus do not produce images. Instead, fiber photometry measures “bulk fluorescence”, or the averaged signal obtained local to the fiberoptic tip, including the contributions of hundreds or thousands of biosensor-expressing cells. Fiber photometry was originally developed for recording neuronal

activity using fluorescent calcium indicators [10-12], and its subsequent popularity has led to the development of commercially available "plug and play" systems for this purpose. In particular the capacity to pair photometric recording with behavioral measures has made it a particularly useful tool to study the neural circuits underlying behavior [5, 13]. Compared to *imaging* technologies such as head-mounted mini-scopes or head-fixed microscopy, fiber photometry is also less invasive, allows access to structures deep in the brain without tissue resection, and permits the simultaneous recording of multiple brain sites, or multiple animals [14].

We have recently described the application of a two-color fiber photometry system to record G protein-coupled receptor (GPCR) dependent signaling pathways *in vivo* using FRET-based biosensors [8]. Using this technique, we measured drug-evoked intracellular signaling in the striatum of Parkinsonian rats to reveal changes in dopamine receptor signaling that occur during chronic treatment with L-DOPA. This approach leverages the existing suite of FRET-based biosensors and represents a powerful tool for studying intracellular signaling, circuit function and pharmacology. In the present article we will describe the general approach and technical considerations for performing fiber photometry with FRET biosensors.

2. Overview of Methods

2.1 Selecting a biosensor

Selecting an appropriate biosensor is a critical first step towards designing an *in vivo* recording experiment. The majority of contemporary fluorescent biosensors can be categorized as either intensity-based or ratiometric [15]. Intensity-based biosensors rely on changes in the brightness

of a single fluorophore, and common examples include the GCaMP series of calcium indicators [16] and neurotransmitter sensors such as dLight [17] and GRABDA [18]. On the other hand, ratiometric sensors rely on *relative* changes in fluorescence intensity between two fluorophores, most often via FRET [19], and dozens of such biosensors have now been generated [2, 3].

The most common fluorescent protein (FP) pairs used in FRET are variants of cyan (CFP) with yellow (YFP), or variants of green (GFP) with red (RFP). Each pairing offers advantages and disadvantages, relating to their brightness, efficiency of energy transfer or photostability [20]. Red-shifted fluorescent proteins which are excited and fluoresce at longer wavelengths (i.e. GFP-RFP pairs) offer several advantages for *in vivo* application. Notably, long wavelength light sources are less phototoxic and less prone to cause tissue heating or to produce auto-fluorescence from tissue [21], which can contribute to higher background signal in photometry. Furthermore, short wavelength light is more prone to be absorbed and scattered by biological tissues. This means that red light can travel more efficiently through a greater depth of tissue, increasing the collection volume below an implanted fiberoptic probe. Many FRET biosensors are available in either CFP/YFP or GFP/RFP format. Despite the potential advantages of red-shifted FPs, in our experience FRET reporters based on CFP/YFP have been brighter and have a larger dynamic range than analogous sensors based on GFP/RFP. High dynamic range implies both that there is a resistance to saturation, and that a small change in biological signal is translated into a larger change in FRET ratio, allowing for better detection of small signaling events above background, and is a paramount consideration when selecting a biosensor. Looking to the future, optimized sensors based on GFP/RFP FRET may ultimately outperform those based on CFP/YFP in all

respects, but at the time of this writing we have found that the benefits of greater dynamic range outweigh the associated drawbacks of CFP/YFP FRET.

When selecting a biosensor, initial characterization may be performed in cell culture to assess the functionality, or to compare the brightness and dynamic range when multiple biosensors are to be used. If possible, biosensors should be tested in cells derived from the target tissue, as the dynamic range of the signaling processes to be measured may be cell-type dependent and it useful to understand the cellular context to optimize biosensor measurements. The application discussed below utilizes the PKA biosensor AKAR3-EV (**Fig. 1A**) [22]. In order to validate AKAR-3EV for *in vivo* application in the rat striatum, we first expressed it in primary rat striatal neurons (**Fig. 1C**) and used fluorescence microscopy to measure FRET responses to stimulation with the dopamine D1 receptor agonist SKF 81297 (**Fig. 1B**). Detailed descriptions of our *in vitro* validation were previously reported [8] and in-depth protocols for performing FRET microscopy are available [23].

2.2 *In vivo* expression of FRET biosensors using adeno-associated viral vectors (AAVs)

Due to their flexibility, simplicity and safety, adeno-associated viruses (AAV) are the most widely used vectors for targeted expression of biosensors in the brain [reviewed in [24]]. AAVs have a packaging size limit of approximately 4500 base-pairs, which can accommodate most FRET-based biosensors together with a compact promoter. Many AAV "backbones" are available through online resources such as Addgene. When selecting an AAV expression vector, the choice of promoter is a critical decision in order to ensure optimal expression of the viral cargo in the cell

population of interest. There are often trade-offs between the size (number of base-pairs), cell-type specificity, and strength of a given promoter. Thus, short promoters that drive high level expression (e.g. CMV, CAG and EF1), tend not to be cell-type specific. Promoters that express specifically in neurons (e.g. Syn) are commonly used, providing a middle ground of cell-type specificity with acceptable expression levels (reviewed in [25]). In order to target more specific, molecularly defined cell types, recombinase-dependent expression vectors can be used in combination with a Cre or Flp recombinase that is expressed either using a second virus or in a transgenic Cre driver line [26]. AAV serotype is another factor that can influence the efficiency and specificity of biosensor expression in various tissues and cell types [27].

In the example presented here, we cloned AKAR3-EV into an AAV backbone with a neuron-specific promotor [8, 28] and used AAV serotype 1 to transduce neurons in the dorsal striatum (**Fig. 2A**). We then confirmed that the biosensor expression was localized to neurons in the intended brain region by performing immunofluorescence with the neuronal marker NeuN (**Fig. 2B**).

2.3 Photometry systems for ratiometric FRET

A number of photometry systems have been described by different labs over the past decade, and several are now commercially available. The majority of commercially available systems are designed with excitation sources and filter-sets specified for application with intensity-based indicators such as GCaMP. However, many photometry systems are modular, such that excitation sources and filters can be exchanged. In principle, any photometry system capable of two-color

recording could be suitable for application with FRET biosensors. Generally these systems share a common core design, typically consisting of the following elements:

- light source for fluorescence excitation (LED or laser diode)
- fluorescence detection unit (most often photomultiplier tubes, i.e. PMTs)
- optical filters for both excitation and emission channels
- dichroic mirrors used to separate excitation and emission wavelengths
- data acquisition and control unit
- purpose-built software for different applications

The FRET photometry acquisition system used in our labs (**Fig. 3A**) was designed and built by Labeo Technologies (Montréal, QC, Canada). The light source for excitation of CFP is a laser diode centered at 450 nm with an optical filter at 438 ± 12 nm (Thor Labs). A dichroic mirror with a cut-off wavelength of 458 nm (Thor Labs) separates the excitation and emission channels. For fluorescence detection, another dichroic mirror (cut-off wavelength of 520 nm) is used to split the emissions into CFP and YFP channels. Each detection channel is coupled with an emission filter (483 ± 16 nm for CFP and 547 ± 27 nm for YFP, Thor Labs) and two PMTs (Hamamatsu Photonics) are used to measure fluorescence. PMT signals are amplified with trans-impedance amplifiers and acquired with a data acquisition device (National Instruments) at up to 1 kHz. The acquisition electronics are connected to a computer through a USB port. Both excitation and emission optical pathways are co-aligned and connected to a 400 µm optical fiber which is connected to a 400 µm fiberoptic patch cable (Doric Lens), which can be connected to the animal

directly, or with an intervening rotary joint (Doric Lens). The acquisition user interface provides real-time visualization of the signal and is used to control laser power, acquisition frequency and program the duration and frequency for periodic recordings.

3. Experimental Procedures

The following sections will describe an overview of the surgical procedures, photometry recording, data analysis, and post-mortem histology for an experiment in which biosensors were targeted to the dorsal striatum of adult rats. The required materials along with the suppliers we used will also be listed. General supplies, such as consumables required for surgery, are not listed.

3.1 Stereotaxic surgery: virus injection and probe placement

For further information, detailed protocols for rodent stereotaxic surgery, virus injection and fiberoptic probe implantation have been previously published, including in the following references [6, 29].

Materials:

1) High titer adeno-associated virus (Canadian Neurophotonics Platform – Viral Vector Core)
2) 400 µm diameter fiberoptic probes, 5 mm long for implantation in dorsal striatum (Doric Lens MFC_400/430-0.48_5mm_MF2.5_FLT, 0.4 mm external diameter)
3) Stereotaxic frame (Stoelting)
4) Hand-held micro drill with 0.6mm bit (NeuroStar)
5) Surgical screws (Stoelting)

6) Hamilton syringe with 26-gauge flat tip needle (Hamilton)
7) Stereotaxic microinjection system (NeuroStar)
8) Dental Cement

Procedures:

All procedures were approved by the McGill University Animal Care Committee, in accordance with Canadian Council on Animal Care Guidelines. Male Sprague-Dawley rats (Charles River) weighing 275-300 g were anesthetized and mounted in a stereotaxic frame. Anesthesia was achieved with isoflurane (3% induction, 1% maintenance) mixed with oxygen, and breathing was monitored throughout the duration of surgery. An initial dose of carprofen analgesic (10 mg/kg s.c.) was also provided at the start of surgery. An incision was made along the midline of the scalp and skin was clipped using bulldog clamps in order to expose the skull. The surface of the skull was cleaned in order to visualize bregma and lambda and the angle of the head was adjusted so that the skull was flat and bregma and lambda were at the same height. Stereotaxic arms were zeroed at bregma, and the location of intended virus injection was marked using permanent marker on the surface of the skull by measuring the distance from bregma. Using a hand-held micro drill with a 0.6 mm diameter drill bit, a hole was made in the cranium for viral injection and probe placement. Additional holes were drilled in order to secure 5 stainless steel surgical screws. These holes were at least 5 mm away from the hole intended for probe placement.

Adeno-associated virus (~$5x10^{12}$ viral genomes/ml, kept on ice) was loaded into a Hamilton syringe with 26-gauge needle connected to the stereotaxic side-arms (i.e. micromanipulators).

The syringe was centered above the cranial hole, and slowly lowered to the target depth in the brain. For expression in the dorsal striatum, the tip was located at the following coordinates relative to bregma: +1.2 AP, ±2.7 ML and -5.5 DV. AAV was injected at a volume of 1 µl and a rate of 0.2 µl/min. After completion of the injection, the syringe was left in place for 10 min and then slowly removed. A 5 mm long optic probe (see materials) with metal ferrule was then fastened to a stereotaxic side-arm and slowly lowered along the same path to target coordinates 0.5 mm dorsal to the virus injection site (+1.2 AP, ±2.7 ML and -5.0 DV). This placement ensures that the light-collection area of the probe includes the center of viral expression. Once the probe is in place, the base of the metal ferrule should be flush with the skull, so it is important to have optic probes of the correct length to target the brain region of interest. Once the optical probe was in place, the skull, together with the inserted surgical screws, were gently cleaned, and dental cement was used to secure the probe and to cover the screws. The dental cement was smoothened at its margins, so as to eliminate any sharp ridges that could irritate the animal. Rats received postoperative monitoring and were administered additional doses of carprofen analgesic (10 mg/kg s.c.) every 24 hours for 3 days after surgery.

3.2 Photometry recording and data analysis

Materials:

1) Fiber photometry recording system with appropriate excitation source and filter set (Labeo Technologies)

2) Rats implanted with an optic probe and expressing a FRET biosensor in the desired brain region (AKAR3-EV expressed in dorsal striatum)
3) Rats implanted with an optic probe and expressing a negative control FRET biosensor in the desired brain region (AKARctl expressed in dorsal striatum)
4) Rats implanted with an optic probe *without* biosensor expression in the desired brain region (probe only in dorsal striatum)
5) Drug and vehicle control (SKF 81297 HBr [Toronto Research Chemicals], 0.9% saline)
6) Testing chamber or arena
7) Fiberoptic patch cord (Doric Lens - MFP_400/430/LWMJ-0.48_0.5m_FCM-FCM)
8) Ceramic mating sleeve (Doric Lens)
9) Fiberoptic rotary joint (optional, depending on setup – Doric Lens)
10) Testing arena (Square plexiglass chamber, 60 x 60 x 60 cm, with a hole in the lid for the patch cord to pass through)

Procedures:

Following recovery from surgery, rats were left undisturbed in their home cages for 3 weeks in order to allow for virus expression. This timeframe was determined both by immunohistochemistry and by monitoring fluorescence signal detected by photometry (**Fig. 3B**). While timing may vary depending on the specific viral construct, we have found that a significant fluorescence signal is detectable between 2-3 weeks after surgery, and we have performed experiments in rats lasting up to 12 weeks with stable fluorescent signal.

Prior to performing the first photometric recording, rats were handled for 5 days and connected to a “dummy” cable in the test cage, in order to acclimatize them to the sensation of being connected to a fiberoptic patch cord. For testing rats in particular, the use of a reinforced optic patch cord with metal jacket is recommended (e.g. Doric LWMJ protective jacket), as unprotected optic fiber can easily be damaged by chewing or grabbing. Experiments described here also utilize a fiberoptic rotary joint (Doric Lens) to allow animals to freely rotate. More generally, a rotary joint will tend to attenuate the signal and is not always needed, depending on the experimental setup and duration of testing.

At the time of recording, rats were placed in the test chamber and the photometry system patch cable was connected to the surgically implanted optic probe using a ceramic mating sleeve (Doric Lens). The excitation source was then turned on and baseline recordings of at least 10 min were acquired prior to drug administration. All photometry recording was performed using laser power of 20 µW and with PMT gain set to 70% for both the CFP and YFP channels. Note that the excitation power level and gain required to generate a robust signal may need to be experimentally determined. Excitation power should be kept as low as possible in order to minimize sensor bleaching, background autofluorescence and tissue heating. Increasing the PMT gain will increase the detection sensitivity, but it is important to avoid saturation. The signal strength from individual animals can vary depending on the accuracy of probe placement, so it is recommended that gain be set such that animals with the largest signal are not saturating, and to leave this value constant across all animals. In order to determine whether a robust signal is detected, the fluorescence intensity should be compared to control rats which have not been

injected with virus. In our experience, signal from sensor-expressing animals should be at least 3-fold greater than control animals.

An example of raw fluorescent signals of CFP and YFP acquired at 1 Hz is shown in **Fig. 3C**, together with the corresponding FRET ratio values. To minimize potential bleaching or photo-toxicity in long-lasting recordings, the laser was turned on for only 30 out of every 60 seconds (i.e. 50% duty cycle), creating a time-resolved series of 30-second 1Hz recordings (**Fig. 3D**). In this example, a single rat expressing the AKAR3-EV biosensor in the dorsal striatum received a systemic injection of either saline or the dopamine D1 receptor agonist SKF 81297 (5 mg/kg), in test sessions one day apart. Note that the choice of drug concentration, vehicle and injection volume will need to be determined based on the solubility of the compound being tested. While many drugs (including SKF 81297) are more soluble in DMSO-containing vehicle than aqueous solution, metabolism of DMSO (which is itself essentially odorless) produces a notable odor that can be detected by rodents; hence, DMSO should be avoided when possible for *in vivo* experiments. More generally, if solvents such as DMSO are required, the concentration should be minimized in order to avoid potential pharmacological actions, or even toxic effects at higher concentrations. For rats, best practices are to limit systemic injection volume to 1 ml of injectate per kg body weight. SKF 81297 is soluble in physiological saline at 5 mg/ml, and thus no added solvent was required. Drugs should be prepared fresh whenever possible. Otherwise, drug solutions should be stored in frozen aliquots at -20 ºC (or colder) and thawed before use, with care taken to ensure that the drug has completely re-dissolved. At the start of testing, a 15-

minute baseline recording was performed and drug was then injected subcutaneously without disconnecting the rat from the photometry system. Injections were performed during a 30 second "laser off" period, as indicated. An increase in FRET ratio can be observed following agonist injection, indicating an increase in PKA activity in the dorsal striatum.

Controls:

For best practice, two types of control recordings are also recommended. The first is to use a control biosensor. This typically consists of a modified version of the FRET biosensor which has been mutated to become unresponsive to cellular signaling. In the case of the PKA sensor AKAR3-EV, the threonine residue phosphorylated by PKA has been mutated to an alanine, locking the control biosensor permanently in the "low FRET" open conformation, unresponsive to agonist stimulation (see **Fig. 1A**). The second type of control is to record from rats that have been implanted with optic probes but do not express any virus. These rats are used to estimate background autofluorescence, which can then be subtracted from FRET recordings during data processing. Recordings from these controls should always be performed in parallel using identical recording parameters as those used in the experimental FRET recordings.

Data processing and analysis:

Data processing for photometry FRET analysis proceeds through the steps outlined in **Figure 4A**. For each recording, we first averaged the CFP and YFP signals from each discrete time bin. In the present example where the laser is turned on for 30 in every 60 seconds, this results in one mean

intensity value per minute. If control recordings from virus-free rats have been performed to measure autofluorescence, these can be used to estimate the autofluorescent contribution to both the CFP and YFP channels at each recording time point. Autofluorescence declines over many minutes, and in our experience this decay can be fitted with a linear equation. In the above example, two control rats were used to calculate the mean background for CFP and YFP channels (**Fig. 4B**). These CFP and YFP mean values were plotted as a function of time and fit to a linear equation which was then used to subtract CFP and YFP background at each time-point from the biosensor recordings. After background subtraction, the FRET ratio was calculated as CFP/YFP. Baseline FRET was calculated as the mean FRET for the pre-injection period and all measurements were subsequently expressed as the percentage ΔFRET relative to baseline FRET [i.e. %ΔF/F = 100*(FRET - $FRET_{baseline}$)/ $FRET_{baseline}$]. The %ΔF/F values for a rat expressing AKAR-EV in the dorsal striatum and treated with either vehicle or D1 dopamine receptor agonist are shown (**Fig. 4C**). While the AKAR-EV expressing rat exhibited a clear drug response, a rat treated in an identical manner expressing a control AKAR-EV biosensor exhibited no response to drug (**Fig. 4D**). These %ΔF/F values can then be averaged across all subjects and subjected to further analysis. In order to perform statistical comparisons on these time-course data we have previously used area-under the curve (AUC) analysis, using the formula shown below, where C is the %ΔF/F value corresponding to each timepoint (T), and B is defined as the mean %ΔF/F of the baseline period [8].

$AUC = 0.5i = \ln{-1}(Ti{+}l{+}Ti)(Ci{+}l{+}Ci{-}2B)$

3.3 Histology to assess virus expression, probe placement and overall tissue integrity

At the completion of all experiments, immunohistochemistry is performed in order to confirm appropriate anatomical location of virus expression and probe insertion, correct cell-type expression of the virus, and assess general integrity of the target tissue (**Fig 2**). Detailed protocols for tissue fixation, immunohistochemistry and imaging are not provided here. In the examples shown, fixation, sectioning and staining were performed as previously described [8]. Briefly, rats were perfused with 4% paraformaldehyde solution, brains were extracted and sectioned using a Vibratome™ (TPI series 1000, Leica Biosystems). Free-floating sections were then permeabilized, blocked and probed with a primary antibody to detect the neuronal marker NeuN (Millipore, MAB377, 1:1000 dilution). A secondary antibody tagged with Alexa fluor-647 (Invitrogen, A21245, 1:500 dilution) and Hoechst 33342 (Thermo Fisher Scientific, H3570, 1:10000 dilution) were then used for fluorescent visualization of NeuN and nuclear DNA, respectively. Sections were then mounted in Fluoromount™ mounting medium (E126367, Invitrogen) and imaged using the Opera Phenix™ High Content microscope (Perkin Elmer) using either a 5x (**Fig. 2A**) or 40x (**Fig. 2B**) objective.

3.6 Troubleshooting

Heterologous expression of transgenes in neurons can in some cases produce toxic effects, especially at very high expression levels. Commercially-produced AAVs often reach viral titers as high as $5x10^{13}$ viral genomes/ml (vg/ml). In our experience, a titer of 1-5 x 10^{12} vg/ml is sufficient for robust biosensor expression in striatal neurons without causing toxicity. However, this may depend on the specific construct, and on the promoter used to drive expression. Viral expression

should be titrated in order to achieve sufficient fluorescence signals, while avoiding potential toxicity. Depending on the size of the region targeted, the extent of viral spread around the injection site must also be considered when determining the titer and volume of injection. Viral injection and transgene expression can disrupt tissue function, even in the absence of cell death. Immunofluorescent staining for cellular markers, as well as behavioral assays sensitive to disruption of the target tissue, can provide reassurance that biosensor expression has not unduly disrupted tissue function.

A potential confounding factor in fiber photometry is the distortion of fluorescence signals by hemodynamic artefacts. Hemoglobin can absorb light in the spectral range used for fluorescent imaging, and this can produce distortions in the fluorescent signal [30]. In our experience we have seen that in a small number of animals, administration of D1R agonists produce a rapid decline in total biosensor fluorescence, which we speculate is due to the ability of D1R stimulation to increase cerebral blood flow [8]. Some computational approaches have been proposed to address the contribution of hemodynamics [30-32], and this is an important consideration in particular when using drugs that alter cerebral blood flow, or when targeting brain regions adjacent to major blood vessels.

Discussion

Here we have described a simple approach for performing *in vivo* optical recording of FRET-based biosensors using fiber photometry. This technique allows intracellular signaling to be recorded in real time from genetically or spatially defined cell populations in the brain and offers a powerful

way to study how intracellular signaling shapes behavior, and how drugs act on signaling pathways in the living brain.

There is now a substantial library of FRET-based fluorescent biosensors. These biosensors, which collectively target dozens of signaling pathways, are generally available to the research community through individual labs or online resources such as Addgene. Recently, these biosensors have seen use in *in vivo* settings, shedding light on how intracellular signaling processes affect behavior and pharmacology [8, 9, 33-38]. While the fiber photometry approach described here represents one approach for measuring FRET *in vivo*, many others have been described, and the choice of technique should be guided by experimental goals. Some examples of alternative approaches include 2-photon intravital imaging [38, 39], or micro-endoscopy with fibered or head-mounted microscopes [33]. These imaging-based techniques offer the advantage of spatial resolution, but are typically much more invasive and costly, and may require physical restraint of the animal. Further, while we have used AAVs to drive biosensor expression in our studies, an alternative approach is the generation of transgenic animals that constitutively or conditionally express a specific biosensor. In fact, several transgenic mouse lines have recently been generated expressing FRET-based reporters including biosensors of PKA and ERK1/2 [33, 35], cAMP [40], and RhoA [38]; these mouse lines can all be used for *in vivo* studies.

Alternative fiber photometry methods for recording the same signaling processes described in this article have also been described. For example, while we have measured FRET as a change in relative fluorescence intensity between the donor and acceptor fluorophores, it can also be

measured by the change in fluorescence lifetime of the donor fluorophore [41]. The latter approach was recently exploited to generate a fiber photometry system for fluorescence lifetime measurement which allowed for sensitive measurement of PKA activity *in vivo* using a FRET-based biosensor [9]. Intensity-based PKA biosensors composed of a single fluorophore have also been generated and can be used in *in vivo* [42]. Such intensity-based sensors are generally compatible with fiber photometry systems already used for GCaMP recording. An advantage of these lifetime or single-fluorophore approaches is that they require detection of only a single wavelength, offering the potential for multiplexed recording with multiple biosensors [15].

In this article, we have described methodological details and technical considerations for ratiometric fiber photometry for monitoring intracellular signaling in freely moving animals using FRET-based biosensors. The system described here can in principle be paired with any FRET-based biosensor, opening the door to *in vivo* detection of dozens of signaling pathways. Due to its simplicity and flexibility, we believe this technique has the potential for application across a broad spectrum of neuroscience research, ranging from the study of neural circuits and behavior, to preclinical drug development and screening.

CRediT author statement

Jace Jones-Tabah: Conceptualization, Methodology, Investigation, Writing – Original Draft. **Hanan Mohammad:** Investigation, Writing – Review & Editing. **Paul B.S. Clarke:**

Conceptualization, Supervision, Writing – Review & Editing. **Terence E. Hébert:** Conceptualization, Supervision, Writing – Review & Editing.

Declaration of Competing Interest

The authors declare that they have no known competing financial interest or personal relationships that could have influenced the work reported here.

Acknowledgements

This work was supported by grants from the Weston Brain Institute and CIHR to P.B.S.C. and T.E.H. J.J.T was supported by doctoral studentships from the CIHR and the McGill Healthy Brains for Healthy Lives initiative. T.E.H. holds the Canadian Pacific Chair in Biotechnology. We thank Dr. Michiyuki Matsuda (Kyoto University) for providing us with biosensor constructs and Dr. Hiroyuki Hioki (Kyoto University) for providing AAV plasmids. We thank the McGill Pharmacology and Therapeutics Imaging and Molecular Biology platform, as well as the McGill Advanced BioImaging Facility for training and assistance with microscopy and image analysis, and the McGill Comparative Medicine and Animal Resource Centre for assistance with animal husbandry and welfare.

Figure Legends:

Fig. 1. Detecting PKA activation in primary neurons using a FRET biosensor. A) Schematic depiction of the PKA biosensor AKAR-EV. Phosphorylation of the biosensor by PKA results in a conformational change that increases energy transfer, and can be detected as an increase in FRET ratio. B) Time course of PKA activation in primary striatal neurons following stimulation with the D1 dopamine receptor agonist SKF 81297 (1 µM), measured using AKAR-EV. C) Representative images of primary striatal neurons expressing AKAR-EV. Images were acquired by exciting the donor CFP, and imaging the emission of both CFP and YFP, demonstrating energy transfer from the donor to acceptor.

Fig. 2. Neuron-specific expression of AKAR-EV in rat dorsal striatum. A) Representative images of AKAR expressed in dorsal striatum under the control of the synapsin promotor. The tract of an optic probe implanted into the virus-expressing region of the dorsal striatum is also visible. B) Representative images of individual AKAR expressing neurons in the dorsal striatum. AKAR-EV was detected by YFP fluorescence (green), while neuronal cell bodies were labelled with NeuN (purple) and total nuclei were labelled with Hoechst (blue).

Fig. 3. *In vivo* detection of FRET using fiber photometry. A) Schematic diagram of the fiber photometry system used. B) Time-course of biosensor expression, measured by the fluorescent signal detected by fiber photometry. X-axis indicates the time elapsed following stereotaxic injection of AAV and probe implantation into dorsal striatum. C) Sample CFP, YFP and FRET signals

recorded at 1 Hz from a rat expressing AKAR in dorsal striatum. D) FRET ratio recorded in 30-second intervals from a rat expressing AKAR in dorsal striatum and injected subcutaneously with either saline or SKF 81297 (5 mg/kg). The trace shows the FRET ratio at a 1 Hz sampling rate, with adjacent 30-second "Laser On" intervals joined by a connecting line.

Fig. 4. Data analysis of fiber photometry FRET signals. A) Overview of the steps used in data processing. B) Autofluorescence measured over time from control rats that do not express the biosensor. C) Processed FRET signals for a single rat expressing AKAR in dorsal striatum and injected subcutaneously with saline or SKF 81297 (5 mg/kg) on different occasions. D) Processed FRET signal for a rat expressing the control AKAR-EV, i.e. with substrate threonine mutated to alanine (T/A), in dorsal striatum; this animal was also injected subcutaneously with saline or SKF 81297 (5 mg/kg).

References

[1] A. Miyawaki, Development of Probes for Cellular Functions Using Fluorescent Proteins and Fluorescence Resonance Energy Transfer, Annu Rev Biochem 80(1) (2011) 357-373. https://doi.org/10.1146/annurev-biochem-072909-094736
[2] B. Hochreiter, A. Pardo-Garcia, J.A. Schmid, Fluorescent Proteins as Genetically Encoded FRET Biosensors in Life Sciences, Sensors 15(10) (2015). https://doi.org/10.3390/s151026281
[3] K. Terai, A. Imanishi, C. Li, M. Matsuda, Two Decades of Genetically Encoded Biosensors Based on Förster Resonance Energy Transfer, Cell Structure and Function 44(2) (2019) 153-169. https://doi.org/10.1247/csf.18035
[4] J. Lecoq, N. Orlova, B.F. Grewe, Wide. Fast. Deep: Recent Advances in Multiphoton Microscopy of In Vivo Neuronal Activity, The Journal of Neuroscience 39(46) (2019) 9042. https://doi.org/10.1523/JNEUROSCI.1527-18.2019
[5] C.A. Siciliano, K.M. Tye, Leveraging calcium imaging to illuminate circuit dysfunction in addiction, Alcohol (Fayetteville, N.Y.) 74 (2019) 47-63. https://doi.org/10.1016/j.alcohol.2018.05.013
[6] G. Cui, S.B. Jun, X. Jin, G. Luo, M.D. Pham, D.M. Lovinger, S.S. Vogel, R.M. Costa, Deep brain optical measurements of cell type–specific neural activity in behaving mice, Nature Protocols 9(6) (2014) 1213-1228. https://doi.org/10.1038/nprot.2014.080
[7] L.A. Gunaydin, L. Grosenick, J.C. Finkelstein, I.V. Kauvar, L.E. Fenno, A. Adhikari, S. Lammel, J.J. Mirzabekov, R.D. Airan, K.A. Zalocusky, K.M. Tye, P. Anikeeva, R.C. Malenka, K. Deisseroth, Natural neural projection dynamics underlying social behavior, Cell 157(7) (2014) 1535-51. https://doi.org/10.1016/j.cell.2014.05.017
[8] J. Jones-Tabah, H. Mohammad, S. Hadj-Youssef, L.E.H. Kim, R.D. Martin, F. Benaliouad, J.C. Tanny, P.B.S. Clarke, T.E. Hébert, Dopamine D1 receptor signalling in dyskinetic Parkinsonian rats revealed by fiber photometry using FRET-based biosensors, Scientific Reports 10(1) (2020) 14426. https://doi.org/10.1038/s41598-020-71121-8
[9] S.J. Lee, Y. Chen, B. Lodder, B.L. Sabatini, Monitoring Behaviorally Induced Biochemical Changes Using Fluorescence Lifetime Photometry, Frontiers in Neuroscience 13(766) (2019). https://doi.org/10.3389/fnins.2019.00766
[10] H. Lütcke, M. Murayama, T. Hahn, D.J. Margolis, S. Astori, S.M. Zum Alten Borgloh, W. Göbel, Y. Yang, W. Tang, S. Kügler, R. Sprengel, T. Nagai, A. Miyawaki, M.E. Larkum, F. Helmchen, M.T. Hasan, Optical recording of neuronal activity with a genetically-encoded calcium indicator in anesthetized and freely moving mice, Frontiers in neural circuits 4 (2010) 9. https://doi.org/10.3389/fncir.2010.00009
[11] G. Cui, S.B. Jun, X. Jin, M.D. Pham, S.S. Vogel, D.M. Lovinger, R.M. Costa, Concurrent activation of striatal direct and indirect pathways during action initiation, Nature 494(7436) (2013) 238-242. https://doi.org/10.1038/nature11846
[12] Lisa A. Gunaydin, L. Grosenick, Joel C. Finkelstein, Isaac V. Kauvar, Lief E. Fenno, A. Adhikari, S. Lammel, Julie J. Mirzabekov, Raag D. Airan, Kelly A. Zalocusky, Kay M. Tye, P. Anikeeva, Robert C. Malenka, K. Deisseroth, Natural Neural Projection Dynamics Underlying Social Behavior, Cell 157(7) (2014) 1535-1551. https://doi.org/10.1016/j.cell.2014.05.017

[13] S.L. Resendez, G.D. Stuber, In vivo Calcium Imaging to Illuminate Neurocircuit Activity Dynamics Underlying Naturalistic Behavior, Neuropsychopharmacology 40(1) (2015) 238-239. https://doi.org/10.1038/npp.2014.206
[14] C.K. Kim, S.J. Yang, N. Pichamoorthy, N.P. Young, I. Kauvar, J.H. Jennings, T.N. Lerner, A. Berndt, S.Y. Lee, C. Ramakrishnan, T.J. Davidson, M. Inoue, H. Bito, K. Deisseroth, Simultaneous fast measurement of circuit dynamics at multiple sites across the mammalian brain, Nature Methods 13(4) (2016) 325-328. https://doi.org/10.1038/nmeth.3770
[15] X. Zhou, S. Mehta, J. Zhang, Genetically Encodable Fluorescent and Bioluminescent Biosensors Light Up Signaling Networks, Trends in Biochemical Sciences 45(10) (2020) 889-905. https://doi.org/10.1016/j.tibs.2020.06.001
[16] S. Mehta, Y. Zhang, R.H. Roth, J.-F. Zhang, A. Mo, B. Tenner, R.L. Huganir, J. Zhang, Single-fluorophore biosensors for sensitive and multiplexed detection of signalling activities, Nature cell biology 20(10) (2018) 1215-1225. https://doi.org/10.1038/s41556-018-0200-6
[17] T. Patriarchi, J.R. Cho, K. Merten, M.W. Howe, A. Marley, W.-H. Xiong, R.W. Folk, G.J. Broussard, R. Liang, M.J. Jang, H. Zhong, D. Dombeck, M. von Zastrow, A. Nimmerjahn, V. Gradinaru, J.T. Williams, L. Tian, Ultrafast neuronal imaging of dopamine dynamics with designed genetically encoded sensors, Science 360(6396) (2018) eaat4422. https://doi.org/10.1126/science.aat4422
[18] F. Sun, J. Zeng, M. Jing, J. Zhou, J. Feng, S.F. Owen, Y. Luo, F. Li, H. Wang, T. Yamaguchi, Z. Yong, Y. Gao, W. Peng, L. Wang, S. Zhang, J. Du, D. Lin, M. Xu, A.C. Kreitzer, G. Cui, Y. Li, A Genetically Encoded Fluorescent Sensor Enables Rapid and Specific Detection of Dopamine in Flies, Fish, and Mice, Cell 174(2) (2018) 481-496.e19. https://doi.org/10.1016/j.cell.2018.06.042
[19] I.T. Li, E. Pham, K. Truong, Protein biosensors based on the principle of fluorescence resonance energy transfer for monitoring cellular dynamics, Biotechnology Letters 28(24) (2006) 1971-1982. https://doi.org/10.1007/s10529-006-9193-5
[20] S.G. Olenych, N.S. Claxton, G.K. Ottenberg, M.W. Davidson, The Fluorescent Protein Color Palette, Current Protocols in Cell Biology 33(1) (2006) 21.5.1-21.5.34. https://doi.org/10.1002/0471143030.cb2105s33
[21] N.C. Deliolanis, R. Kasmieh, T. Wurdinger, B.A. Tannous, K. Shah, V. Ntziachristos, Performance of the red-shifted fluorescent proteins in deep-tissue molecular imaging applications, J Biomed Opt 13(4) (2008) 044008. https://doi.org/10.1117/1.2967184
[22] N. Komatsu, K. Aoki, M. Yamada, H. Yukinaga, Y. Fujita, Y. Kamioka, M. Matsuda, Development of an optimized backbone of FRET biosensors for kinases and GTPases, Molecular biology of the cell 22(23) (2011) 4647-56. https://doi.org/10.1091/mbc.E11-01-0072
[23] J.A. Broussard, B. Rappaz, D.J. Webb, C.M. Brown, Fluorescence resonance energy transfer microscopy as demonstrated by measuring the activation of the serine/threonine kinase Akt, Nature protocols 8(2) (2013) 265-281. https://doi.org/10.1038/nprot.2012.147
[24] D.L. Haggerty, G.G. Grecco, K.C. Reeves, B. Atwood, Adeno-Associated Viral Vectors in Neuroscience Research, Molecular therapy. Methods & clinical development 17 (2020) 69-82. https://doi.org/10.1016/j.omtm.2019.11.012
[25] L. Haery, B.E. Deverman, K.S. Matho, A. Cetin, K. Woodard, C. Cepko, K.I. Guerin, M.A. Rego, I. Ersing, S.M. Bachle, J. Kamens, M. Fan, Adeno-Associated Virus Technologies and

Methods for Targeted Neuronal Manipulation, 13(93) (2019).
https://doi.org/10.3389/fnana.2019.00093
[26] L.E. Fenno, J. Mattis, C. Ramakrishnan, K. Deisseroth, A Guide to Creating and Testing New INTRSECT Constructs, Curr Protoc Neurosci 80 (2017) 4.39.1-4.39.24.
https://doi.org/10.1002/cpns.30
[27] A. Watakabe, M. Ohtsuka, M. Kinoshita, M. Takaji, K. Isa, H. Mizukami, K. Ozawa, T. Isa, T. Yamamori, Comparative analyses of adeno-associated viral vector serotypes 1, 2, 5, 8 and 9 in marmoset, mouse and macaque cerebral cortex, Neuroscience Research 93 (2015) 144-157.
https://doi.org/10.1016/j.neures.2014.09.002
[28] J. Sohn, M. Takahashi, S. Okamoto, Y. Ishida, T. Furuta, H. Hioki, A Single Vector Platform for High-Level Gene Transduction of Central Neurons: Adeno-Associated Virus Vector Equipped with the Tet-Off System, PLOS ONE 12(1) (2017) e0169611.
https://doi.org/10.1371/journal.pone.0169611
[29] F. Zhang, V. Gradinaru, A.R. Adamantidis, R. Durand, R.D. Airan, L. de Lecea, K. Deisseroth, Optogenetic interrogation of neural circuits: technology for probing mammalian brain structures, Nature Protocols 5(3) (2010) 439-456. https://doi.org/10.1038/nprot.2009.226
[30] M.T. Valley, M.G. Moore, J. Zhuang, N. Mesa, D. Castelli, D. Sullivan, M. Reimers, J. Waters, Separation of hemodynamic signals from GCaMP fluorescence measured with wide-field imaging, Journal of neurophysiology 123(1) (2019) 356-366.
https://doi.org/10.1152/jn.00304.2019
[31] W. Akemann, H. Mutoh, A. Perron, Y.K. Park, Y. Iwamoto, T. Knöpfel, Imaging neural circuit dynamics with a voltage-sensitive fluorescent protein, Journal of neurophysiology 108(8) (2012) 2323-37. https://doi.org/10.1152/jn.00452.2012
[32] Y. Ma, M.A. Shaik, S.H. Kim, M.G. Kozberg, D.N. Thibodeaux, H.T. Zhao, H. Yu, E.M.C. Hillman, Wide-field optical mapping of neural activity and brain haemodynamics: considerations and novel approaches, Philosophical Transactions of the Royal Society B: Biological Sciences 371(1705) (2016) 20150360. https://doi.org/10.1098/rstb.2015.0360
[33] A. Goto, I. Nakahara, T. Yamaguchi, Y. Kamioka, K. Sumiyama, M. Matsuda, S. Nakanishi, K. Funabiki, Circuit-dependent striatal PKA and ERK signaling underlies rapid behavioral shift in mating reaction of male mice, Proceedings of the National Academy of Sciences 112(21) (2015) 6718. https://doi.org/10.1073/pnas.1507121112
[34] T. Hiratsuka, T. Sano, H. Kato, N. Komatsu, M. Imajo, Y. Kamioka, K. Sumiyama, F. Banno, T. Miyata, M. Matsuda, Live imaging of extracellular signal-regulated kinase and protein kinase A activities during thrombus formation in mice expressing biosensors based on Förster resonance energy transfer, Journal of Thrombosis and Haemostasis 15(7) (2017) 1487-1499.
https://doi.org/10.1111/jth.13723
[35] Y. Kamioka, K. Sumiyama, R. Mizuno, Y. Sakai, E. Hirata, E. Kiyokawa, M. Matsuda, Live Imaging of Protein Kinase Activities in Transgenic Mice Expressing FRET Biosensors, Cell Structure and Function 37(1) (2012) 65-73. https://doi.org/10.1247/csf.11045
[36] T. Laviv, B. Scholl, P. Parra-Bueno, B. Foote, C. Zhang, L. Yan, Y. Hayano, J. Chu, R. Yasuda, In Vivo Imaging of the Coupling between Neuronal and CREB Activity in the Mouse Brain, Neuron 105(5) (2020) 799-812.e5. https://doi.org/10.1016/j.neuron.2019.11.028
[37] L. Ma, B.C. Jongbloets, W.-H. Xiong, J.B. Melander, M. Qin, T.J. Lameyer, M.F. Harrison, B.V. Zemelman, T. Mao, H. Zhong, A Highly Sensitive A-Kinase Activity Reporter for Imaging

Neuromodulatory Events in Awake Mice, Neuron 99(4) (2018) 665-679.e5. https://doi.org/10.1016/j.neuron.2018.07.020
[38] M. Nobis, D. Herrmann, S.C. Warren, S. Kadir, W. Leung, M. Killen, A. Magenau, D. Stevenson, M.C. Lucas, N. Reischmann, C. Vennin, J.R.W. Conway, A. Boulghourjian, A. Zaratzian, A.M. Law, D. Gallego-Ortega, C.J. Ormandy, S.N. Walters, S.T. Grey, J. Bailey, T. Chtanova, J.M.W. Quinn, P.A. Baldock, P.I. Croucher, J.P. Schwarz, A. Mrowinska, L. Zhang, H. Herzog, A. Masedunskas, E.C. Hardeman, P.W. Gunning, G. del Monte-Nieto, R.P. Harvey, M.S. Samuel, M. Pajic, E.J. McGhee, A.-K.E. Johnsson, O.J. Sansom, H.C.E. Welch, J.P. Morton, D. Strathdee, K.I. Anderson, P. Timpson, A RhoA-FRET Biosensor Mouse for Intravital Imaging in Normal Tissue Homeostasis and Disease Contexts, Cell Reports 21(1) (2017) 274-288. https://doi.org/10.1016/j.celrep.2017.09.022
[39] R.N. Day, W. Tao, K.W. Dunn, A simple approach for measuring FRET in fluorescent biosensors using two-photon microscopy, Nature Protocols 11(11) (2016) 2066-2080. https://doi.org/10.1038/nprot.2016.121
[40] B.S. Muntean, S. Zucca, C.M. MacMullen, M.T. Dao, C. Johnston, H. Iwamoto, R.D. Blakely, R.L. Davis, K.A. Martemyanov, Interrogating the Spatiotemporal Landscape of Neuromodulatory GPCR Signaling by Real-Time Imaging of cAMP in Intact Neurons and Circuits, Cell Rep 22(1) (2018) 255-268. https://doi.org/10.1016/j.celrep.2017.12.022
[41] W. Becker, Fluorescence lifetime imaging – techniques and applications, Journal of Microscopy 247(2) (2012) 119-136. https://doi.org/10.1111/j.1365-2818.2012.03618.x
[42] J.-F. Zhang, B. Liu, I. Hong, A. Mo, R.H. Roth, B. Tenner, W. Lin, J.Z. Zhang, R.S. Molina, M. Drobizhev, T.E. Hughes, L. Tian, R.L. Huganir, S. Mehta, J. Zhang, An ultrasensitive biosensor for high-resolution kinase activity imaging in awake mice, Nature Chemical Biology 17(1) (2021) 39-46. https://doi.org/10.1038/s41589-020-00660-y